LASER INTERFEROMETER GRAVITATIONAL WAVE OBSERVATORY
– LIGO –

LIGO Laboratory / LIGO Scientific Collaboration

LIGO-T010140-01-D 3 December 2001

Digital Suspension Filter Design

P Fritschel

Distribution of this draft:

This is an internal working note
of the LIGO Project.

California Institute of Technology
LIGO Project - MS 51-33
Pasadena CA 91125
Phone (818) 395-2129
Fax (818) 304-9834
E-mail: info@ligo.caltech.edu

Massachusetts Institute of Technology
LIGO Project - NW17-161
Cambridge, MA 01239
Phone (617) 253-4824
Fax (617) 253-7014
E-mail: info@ligo.mit.edu

LIGO Hanford Observatory
P.O. Box 1970
Mail Stop S9-02
Richland, WA 99352
Phone 509-372-8106
Fax 509 372 8137

LIGO Livingston Observatory
P.O. Box 940
Livingston, LA 70754
Phone 225-686-3100
Fax 225-686-7189

http://www.ligo.caltech.edu/

1 INTRODUCTION

This document presents designs for the digital suspension controller filters. It covers SOS and LOS optics.

Note: The design that follows relies on some changes to the initial suspension controller front end software. In particular, the coordinated switching of hardware and software filters must be modified from the initial controller software version; as of 7 Nov '01, these modifications are still pending.

Version 01:

- *moved the ac-coupling filters, see section 4.2.*
- *added small amount of damping to the output matrix filters for realizibility (section 4.5.)*
- *broke up the SOS low-pass filtering into 2 filter stages; simplified side low-pass filter*

2 SYSTEM DIAGRAM

The digital suspension control system design is described in LIGO-T000073-00-D, *Digital LOS and SOS Control Systems for LIGO*. A simplified block diagram is shown in Figure 1.

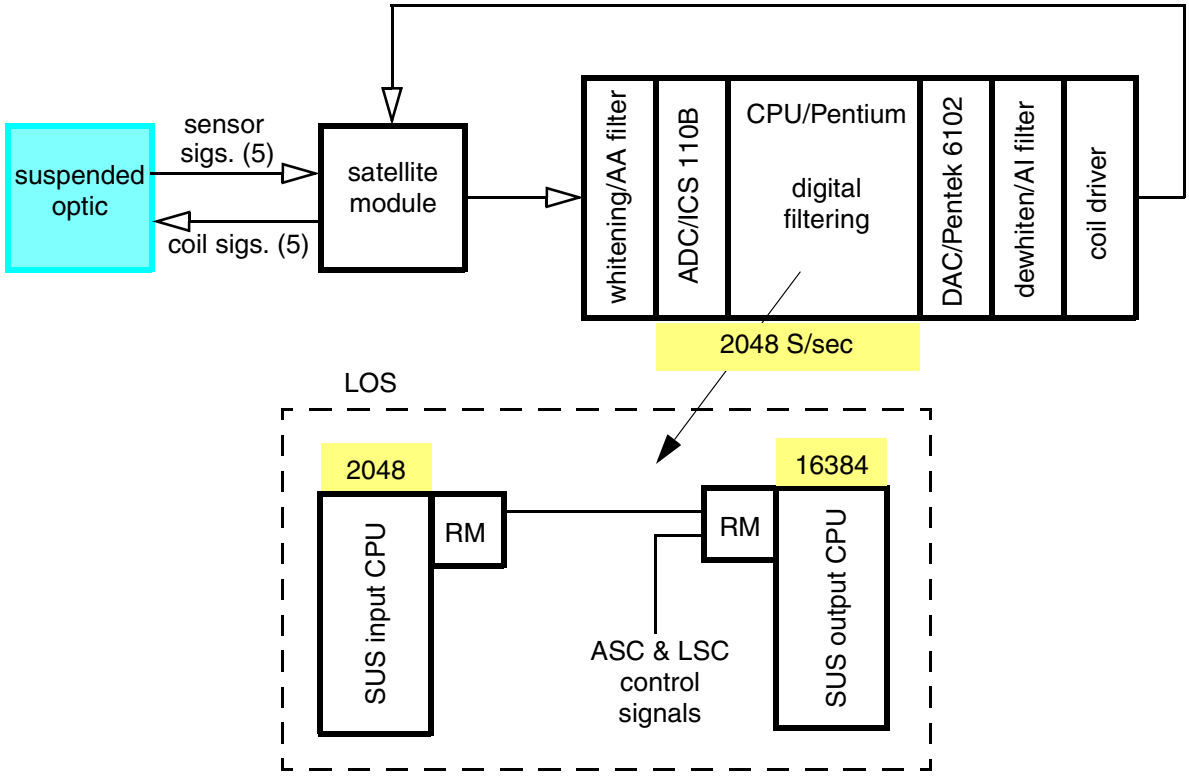

Figure 1. Block diagram of the digital suspension system. For the SOS, a single Pentium CPU processes all suspension signals. For the LOS, one Pentium CPU processes the suspensions' local sensor signals (SUS input CPU), and a second CPU combines these suspension signals with the ASC & LSC signals and performs appropriate output processing (SUS output CPU). The second CPU calculates at the LSC rate of 16,384 S/sec

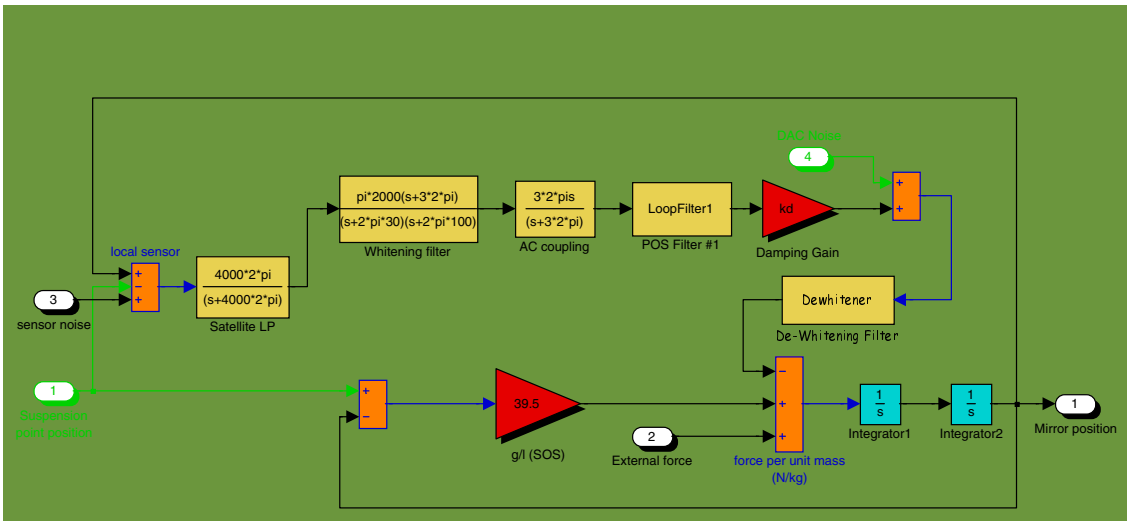

Figure 2. Simulink block diagram of the SOS system. Sensor noise is taken to be $10^{-10}\mathrm{m}/\sqrt{\mathrm{Hz}}$. Suspension point motion is estimated using the Hytec HAM stack model (for SOS) and the following model for ground motion: $10^{-9}\mathrm{m}/\sqrt{\mathrm{Hz}}$ up to 10 Hz, falling as f^{-2} above 10 Hz (clearly an underestimate below 1 Hz). 'LoopFilter1' contains a low-pass filter to reduce sensor noise.

3 SENSOR SIGNAL CONDITIONING

The satellite module D961289-B converts each shadow sensor's photodiode current to a voltage, with a 39.2 kohm transimpedance amplifier (3 dB bandwidth of 4 kHz). At the nominal operating point, the DC photocurrent is about 25 microamp, producing a DC voltage of 1 V. The voltage noise due to shot noise is approximately 110 nV/√Hz; other electronic noise sources are significantly smaller (Johnson noise of the resistor is about 25 nV/√Hz).

The whitening filter (D000210) contains a zero at 3 Hz and poles at 30 Hz and 100 Hz, and has a DC gain of 0 dB. The output of the whitening filter is sent to an ICS 110B ADC module. Figure 3 shows the sensor spectrum in comparison to the ADC noise.

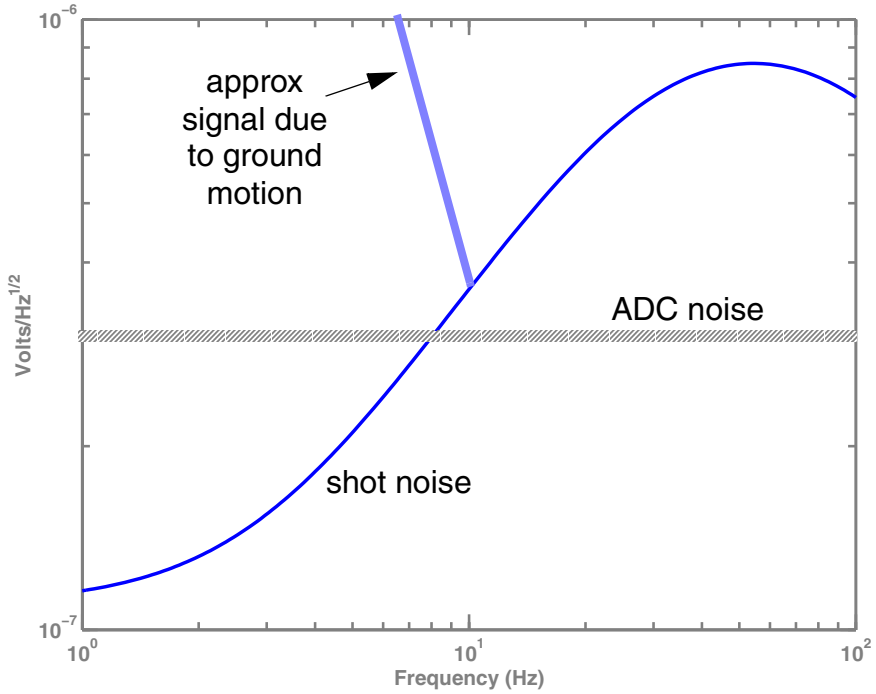

Figure 3. Spectrum of a suspension local sensor (whitening filter output) and ADC noise. The sensor can see ground motion up to approximately 10 Hz, above which it is dominated by shot noise. Input noise of the ICS 110B ADC modules is taken to be 300 nV/rtHz. The sensor signal is above ADC noise at all frequencies, though barely so around 10 Hz.

4 DIGITAL FILTERING

The suspension digital filters are defined in text files, one file per suspended optic. Each selectable filter is labeled by a number, and is defined in second-order-section form; each filter can contain up to four second-order-sections, with filter coefficients given in the following order:

$$\begin{array}{ccccc} g & a_{11} & a_{12} & b_{11} & b_{12} \\ & a_{21} & a_{22} & b_{21} & b_{22} \\ & a_{31} & a_{32} & b_{31} & b_{32} \\ & a_{41} & a_{42} & b_{41} & b_{42} \end{array}$$

where the z-domain transfer function is:

$$H(z) = g\left(\frac{1 + b_{11}z^{-1} + b_{12}z^{-2}}{1 + a_{11}z^{-1} + a_{12}z^{-2}}\right)\cdots\left(\frac{1 + b_{41}z^{-1} + b_{42}z^{-2}}{1 + a_{41}z^{-1} + a_{42}z^{-2}}\right)$$

Filter numbers are indicated in Figure 4.

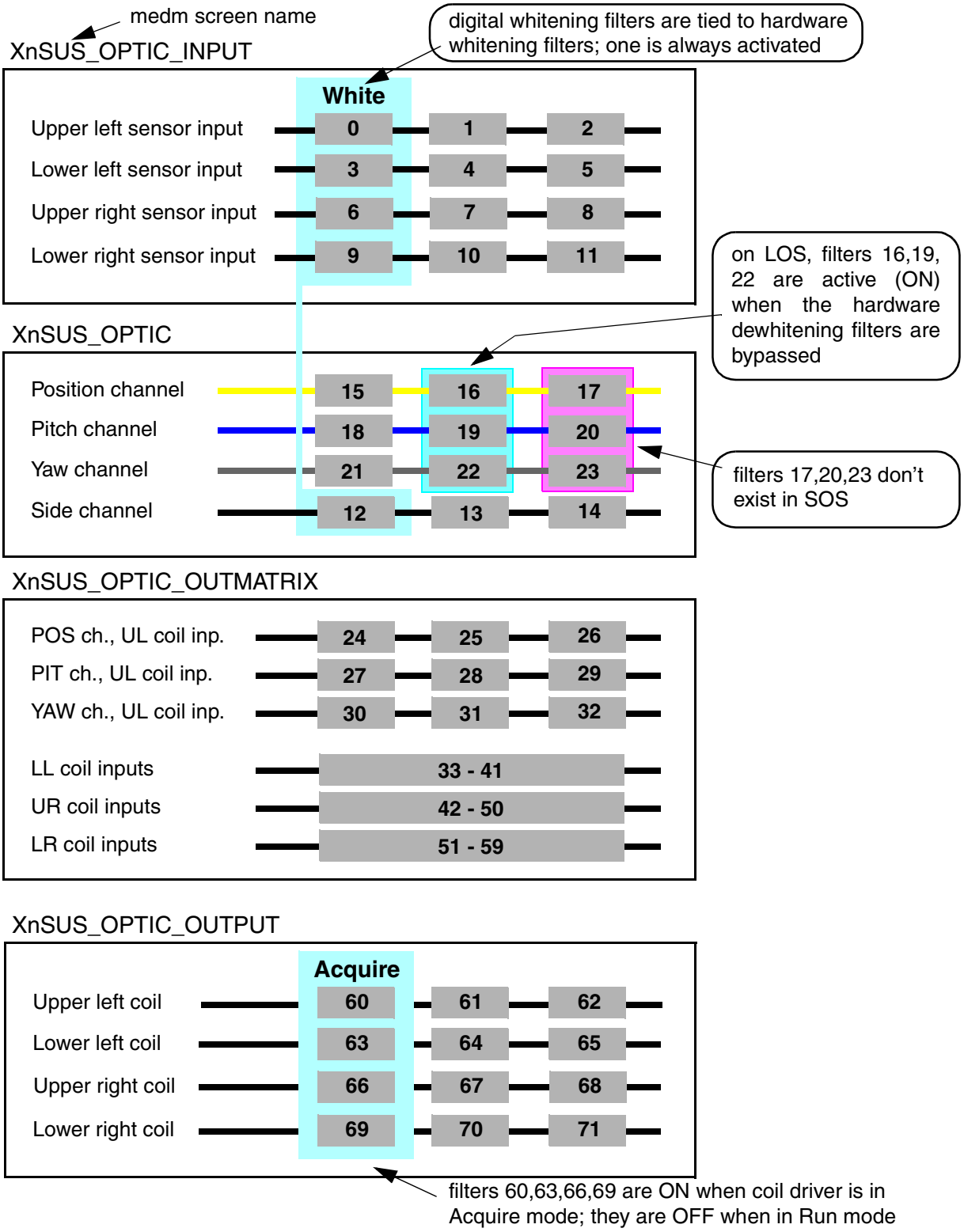

Figure 4. Identification numbers for the digital filters selectable in the four suspension controller screens. As indicated, several filters and filter groups are tied to corresponding switching of hardware filters.

4.1. Sensor filtering

The first filter in each sensor path is labeled ‘White’, and is identical to the hardware whitening filter: a zero at 3 Hz, and poles at 30 Hz and 100 Hz. These filters (numbers 0, 3, 6, 9 and 12) are controlled in conjunction with the hardware whitening filters (and vice-versa): one of the two filters is always activated. Normal operation is to activate the hardware whitening filters, so that the digital whitening filters are inactive.

4.2. AC coupling

The second filter in each sensor path (filters 1, 4, 7 & 10) is an ac-coupling filter: a zero at DC and a pole at 3 Hz. In combination with the whitening filters, each channel is thus differentiated up to 30 Hz. For the side channel filter 13 provides the ac-coupling.

Previously, this filter had been the first filter in the POS, PIT, and YAW paths. This was after the adjustable damping gain, and it was found that the transient from the filter step response could disrupt the mode cleaner lock.

4.3. Low pass filtering, SOS

Following the ac-coupling, the damping signals must be low-pass filtered so that sensor noise does not compromise the stability of the suspended optic. The low-pass filter is designed with the following criteria:

- In the GW band ($f > 40$ Hz), sensor noise must be significantly below the displacement noise requirement for the optic. The MC mirrors are the most critical SOS: the frequency noise requirement of $10^{-3}\,\mathrm{Hz}/\sqrt{\mathrm{Hz}}$ at 40 Hz corresponds to a individual mirror noise of $3\times10^{-17}\,\mathrm{m}/\sqrt{\mathrm{Hz}}$. Sensor noise is allowed to contribute at a level of no more than $10^{-17}\,\mathrm{m}/\sqrt{\mathrm{Hz}}$.
- In the control band ($f < 40$ Hz), sensor noise should come in lower than ground noise.
- The system must be stable for damping gains corresponding to quality factors $Q \geq 3$.
- At the nominal $Q = 10$ damping gain, the transfer function from force applied to the suspended optic to optic motion must not deviate significantly from that of an ideal pendulum with this quality factor.

The last two criteria constrain the low-pass filter from being overly agressive. The following combination of filters is found to meet these criteria:

- an 2nd order elliptic low-pass, with $f_c = 3$ Hz, 0.1 dB passband ripple, stopband of –20 dB
- a stopband filter, which rolls off from 9-30 Hz with 4 complex poles and 4 complex zeros, then comes back up from 35-60 Hz with another 4 complex zeros and poles

The filter response and the noise levels predicted by the model of Figure 2 are shown in Figure 5. This shows that DAC noise, assumed to be $3\ \mu\mathrm{V}/\sqrt{\mathrm{Hz}}$, dominates the noise budget for frequencies above ~15 Hz, and is above the 40 Hz, $10^{-17}\,\mathrm{m}/\sqrt{\mathrm{Hz}}$ requirement. An additional factor of 10 filtering may be realized by moving a 0.1 Hz pole/1 Hz zero filter from the mode cleaner servo to the MC coil driver (and providing a compensating digital filter); though the 40 Hz noise requirement is then met, DAC noise still dominates in the band ~20-40 Hz, as shown in Figure 5.

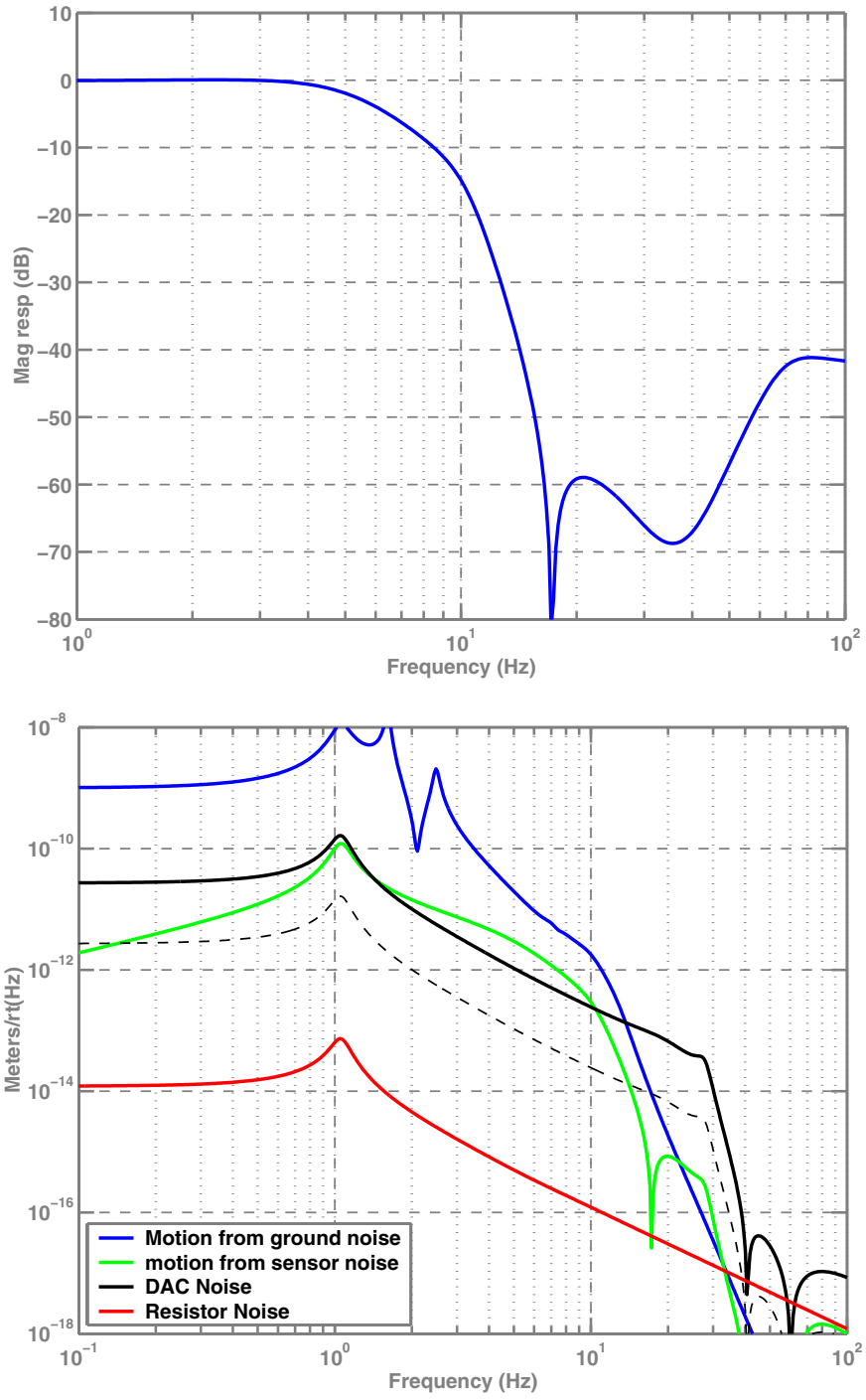

Figure 5. Top: Magnitude response of the digital low-pass filter used to remove sensor noise. Bottom: Displacement noise levels from various sources for a pendulum $Q = 7$. 'Resistor noise' is the Johnson noise from the 1.2 kohm series resistors used in each MC mirror coil driver. The dashed black line is the DAC noise with 10x additional analog filtering (from a 0.1 Hz pole, 1 Hz zero).

The step response and transfer functions are shown in Figure 6–Figure 8.

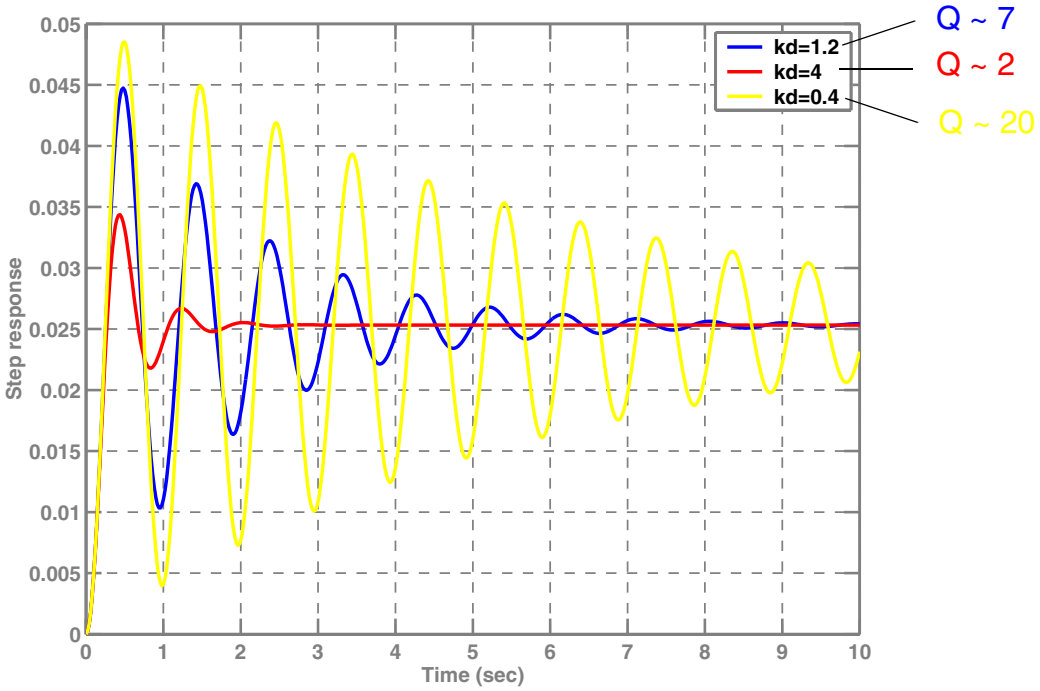

Figure 6. Step response of the optic position to a force input, for different values of damping gain.

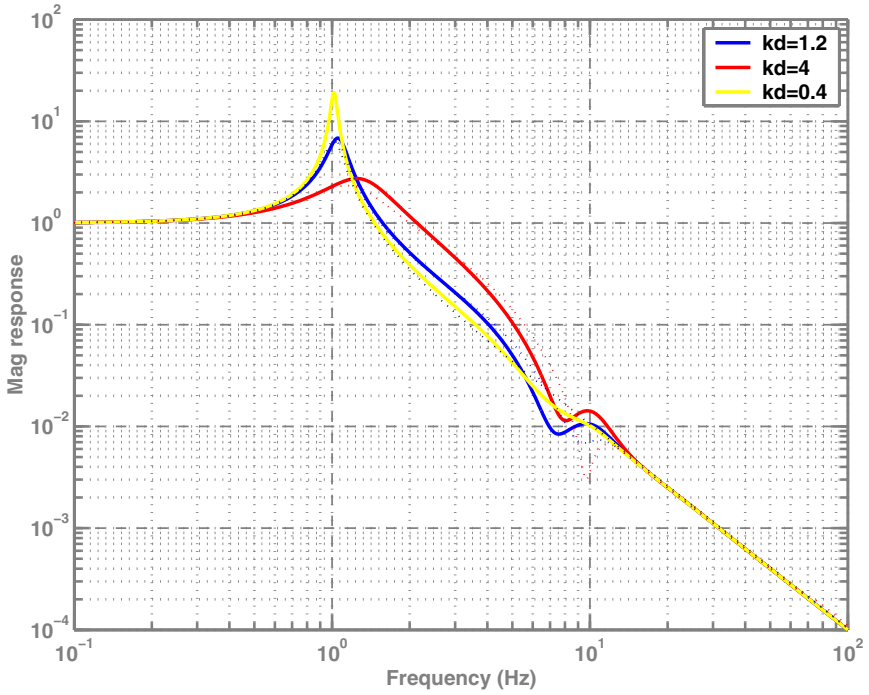

Figure 7. Transfer function of suspension point motion to optic motion, for various damping gains, and with/without the analog dewhitening filter engaged. The colored dashed lines are without the dewhitening filter; the black dashed line is a simple $Q = 7$ resonance for comparison.

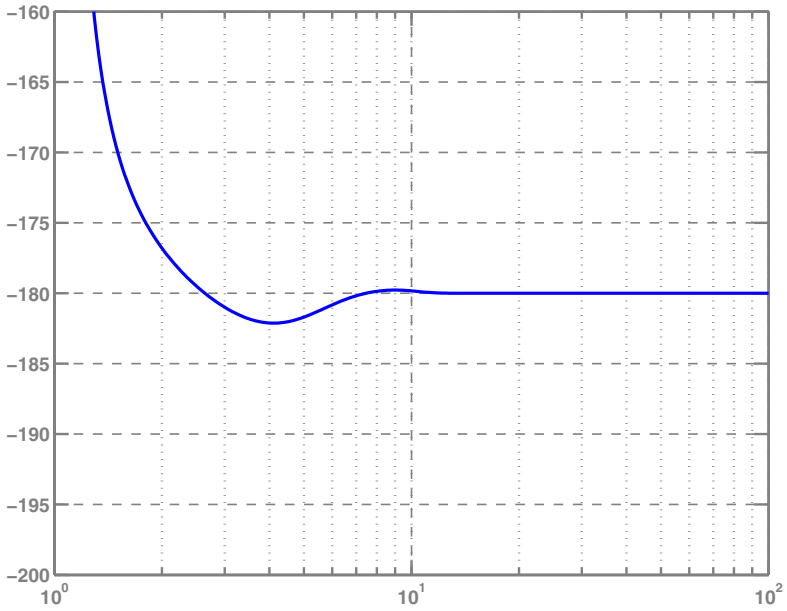

Figure 8. Phase of the force-to-displacement transfer function, with digital elliptic low-pass filter and analog dewhitening filters engaged, and damping gain set for $Q = 7$. This shows that the deviation from an ideal asymptotic fall to −180° is minimal.

The filter combination given above takes 5 second-order-sections to realize digitally. Since the DSC code allows for 4 s.o.s. per filter stage, the filters are broken up as follows:

filter number	*filter loaded*
15, 18, 21	2nd order elliptic low-pass, with $f_c = 3$ Hz, 0.1 dB passband ripple, stopband of –20 dB
16, 19, 22	9-30 Hz 4th order stopband filter

For the pitch and yaw damping paths, we simply use the same low-pass filter. The side path has one less filter stage available, but it does not need as much attenuation. So for the side channel, the stopband filter is made 3rd order.

4.4. Low-pass filtering, LOS

The LOS system has additional modes of operation to consider in the low-pass filter design: with/without analog dewhitening filters; RUN/ACQUIRE modes of the coil drivers. The following requirements are imposed in this case:

- when the dewhitening filter is bypassed, the local sensor noise should be below ground noise and DAC noise, in both RUN and ACQUIRE modes
- when the Test Mass suspensions are in detection mode (dewhitening filters engaged, RUN mode selected), their position local damping is turned off (damping signals come from the

interferometer signals); thus there is no local sensor noise requirement in this mode for the test masses

- the detection mode of the auxiliary core optics (RM, BS, FMs) is with dewhitening filters engaged, and ACQUIRE mode selected for the coil driver; since the interferometer is approximately 100× less sensitive to the auxiliary optics than to the test masses, the sensor noise requirement in this mode is set to $< 10^{-17}\,\mathrm{m}/\sqrt{\mathrm{Hz}}$ at 40 Hz (this is 10× above the test mass displacement noise, so that auxiliary optic local sensor noise will be at least 10× below the interferometer's displacement noise level).

4.4.1. LOS dewhitening filter

The LOS dewhitening filter is described in LIGO-T000074-00-D. It is essentially a modified Chebyshev stopband filter, with –70 dB of attenuation from ~40–150 Hz. For the LOS modeling, the poles and zeros of this filter are loaded into the 'Dewhitener' block of Figure 2.

4.4.2. Coil driver response and noise

The response of the LOS coil driver (D000325-A) is:

$$\frac{I_{\mathrm{coil}}}{V_{\mathrm{in}}} = \frac{1}{470\Omega}\cdot\frac{(s+2\pi\cdot 2.2)}{(s+2\pi\cdot 100)}\cdot\frac{(s+2\pi\cdot 30)}{(s+2\pi\cdot 4.4)}\cdot\left(\frac{100\cdot 4.4}{2.2\cdot 30}\right) \quad \text{ACQUIRE mode}$$
$$\frac{I_{\mathrm{coil}}}{V_{\mathrm{in}}} = \frac{1}{470\Omega}\cdot\frac{(s+2\pi\cdot 30)}{(s+2\pi\cdot 4.4)}\cdot\left(\frac{4.4}{30}\right) \quad \text{RUN mode} \qquad (1)$$

The coil driver response is compensated by including the inverse as digital filters in the output coil paths, as described later.

Electronics noise in the coil driver is calculated including:

- thermal noise of the input 470 ohm resistor
- thermal noise of the first stage feedback impedance
- current noise (4.7 pA/√Hz) of the first stage LT1125 op-amp (voltage noise is negligible)
- thermal noise of the load impedance (in series with the coil)

4.4.3. Filter design

The following pair of filters is found to meet the performance criteria:

1. 2nd order elliptic low-pass, f_c = 3 Hz, stopband = –20 dB, passband ripple = 0.1 dB; this filter is always engaged
2. 3rd order elliptic low-pass, f_c = 5 Hz, stopband = –40 dB, passband ripple = 0.1 dB; this filter is engaged when the hardware dewhitening filter is disengaged

Magnitude responses of these filters are shown in Figure 9.

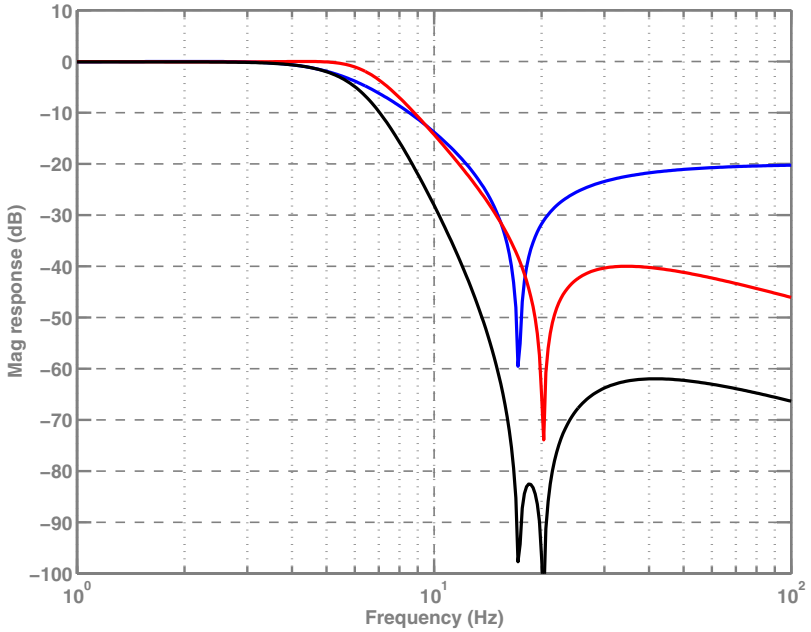

Figure 9. Low-pass filters used in the LOS damping paths to remove local sensor noise. Blue: filter used in all modes; Red: additional filter used when the analog dewhitening filter is bypassed; Black: combined response of the two filters.

4.4.4. Displacement noise

The displacement noise levels for the LOS predicted by the model are shown in Figure 10. When the DAC dewhitening filters are bypassed, the local sensor path is sufficiently filtered that sensor noise is below DAC noise, in both Run and Acquire modes of the coil driver, as desired. With the dewhitening filter engaged, sensor noise is comparable to DAC noise in Acquire mode, feeding through at a level of about $3\times10^{-18}\,\mathrm{m}/\sqrt{\mathrm{Hz}}$ at 40 Hz. This is sufficiently low for the auxiliary core optics, whereas for the test masses, the POS local damping can be turned off for lowest noise operation.

There may be times during interferometer commissioning when the Test Mass suspensions are operated with less aggressive DAC (analog) dewhitening filters, coil drivers in Run mode, and POS local damping engaged. In this case local sensor noise would be about 30× above DAC noise with the Figure 9 filter. A more aggressive digital filter could be designed for this case, as the need arises.

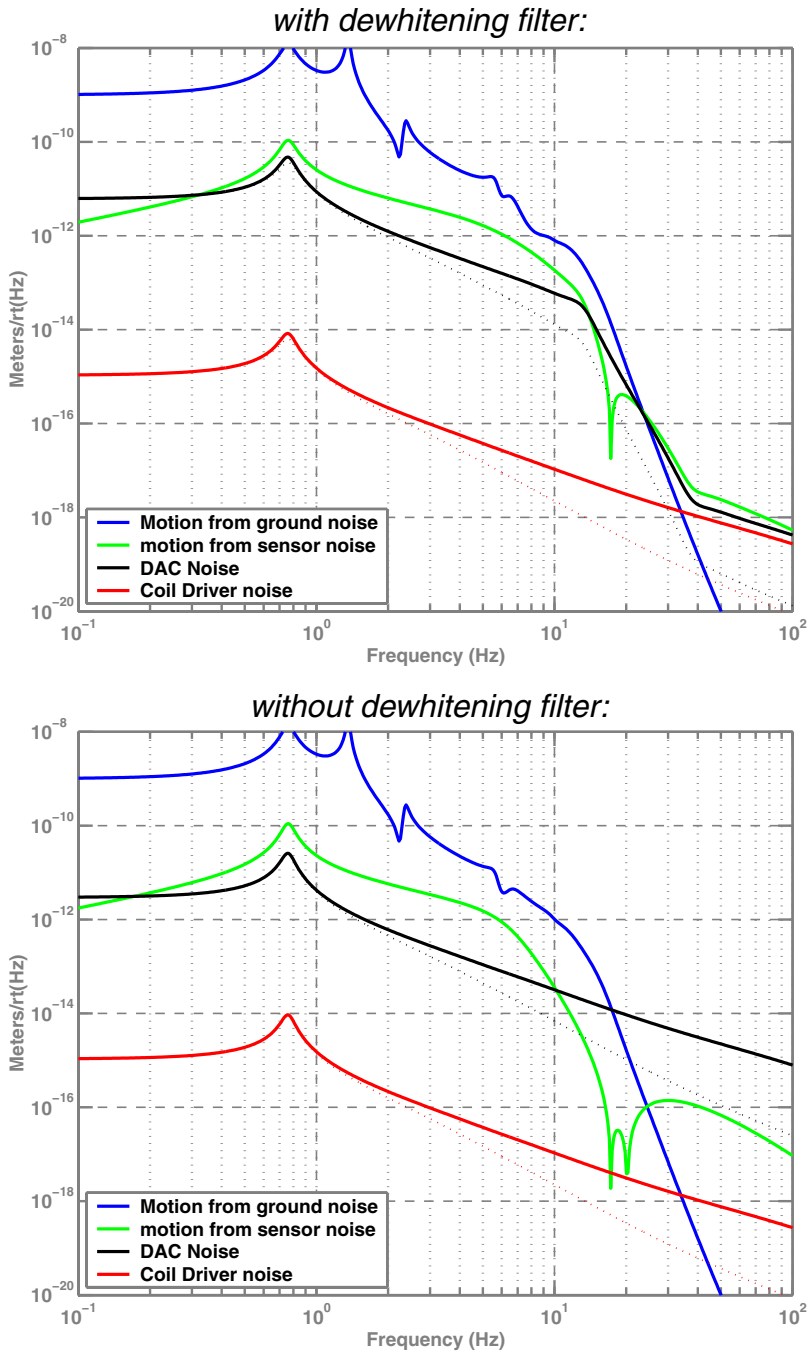

Figure 10. Noise levels in the LOS suspension, with and without the analog dewhitening filter engaged. The black and red dashed lines in each plot are the DAC and coil driver noise, respectively, when the coil driver is in RUN mode (solid lines for ACQUIRE mode). Without the dewhitening filter, local sensor noise is always below DAC noise. With the dewhitening filter, local sensor noise only needs to be below 10^{-17} m/$\sqrt{\text{Hz}}$ at 40 Hz, since the test mass local damping (position) is turned off.

4.4.5. Angular noise

Assuming the same filters are used for the PIT and YAW local damping paths, we can estimate the angular noise due to the local sensors. Since the sensors are approximately 0.1 m from the rotation axes, the vertical axis of Figure 9 can be turned into radians/√Hz by multiplying by 10 rad/m, and dividing by ~2 to account for the lower rotational eigenfrequencies. Thus with the dewhitening filters engaged, sensor noise would produce around 2×10^{-17} rad/$\sqrt{\text{Hz}}$ of angular noise at 40 Hz; this is approximately an order of magnitude above the requirement for ASC control noise (see T952007-04-I, ASC DRD). Thus for lowest noise operation, the PIT & YAW local damping should be turned off as well (all core optics will be controlled via WFS feedback signals), or at least the local damping gain should be reduced by an order of magnitude.

4.4.6. Side channel

Sensor noise from the side channel should be kept below $\sim 10^{-17}$ m/$\sqrt{\text{Hz}}$ at 40 Hz. This is 10× the test mass displacement noise level, and assuming that side motion couples in to optic-axis readout at the 1% level, side local sensor noise would be 1/10 of the test mass displacement.

The LOS side channel coil driver is different from the face channel coil drivers; there is only one mode, which has a frequency independent response of $I_{\text{coil}}/V_{\text{in}} = 1/7150\ \Omega$. The side channel DAC output goes through the same type of dewhitening filter as the face channels; there is no need to bypass the side dewhitening filter during acquisition, so the sensor filtering is designed assuming it is always engaged. A modest low-pass filter of 2 poles at 6 Hz and 2 zeros at 60 Hz does the job, with predicted noise levels shown in Figure 11; this is loaded into filter number 13.

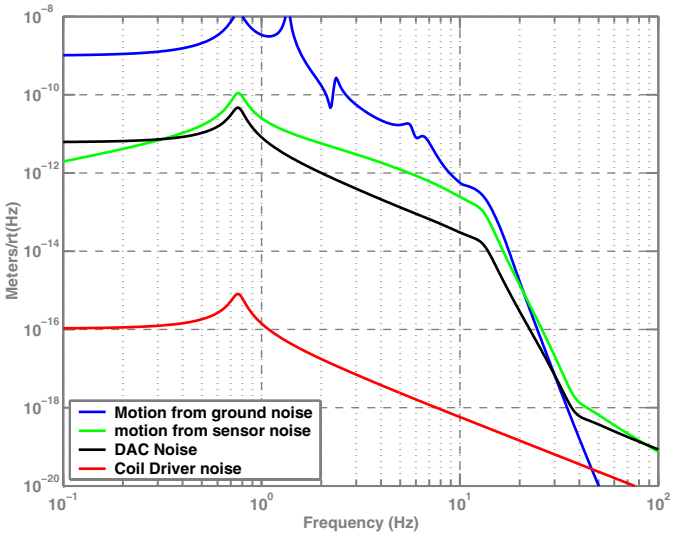

Figure 11. Side (transverse) displacement noise for an LOS. The model includes the DAC dewhitening filter as defined in section 4.4.1., and sensor low-pass filtering of 2 poles at 6 Hz, and 2 zeros at 60 Hz. Sensor noise falls safely below the target of 10^{-17} m/√Hz at 40 Hz.

4.4.7. Response

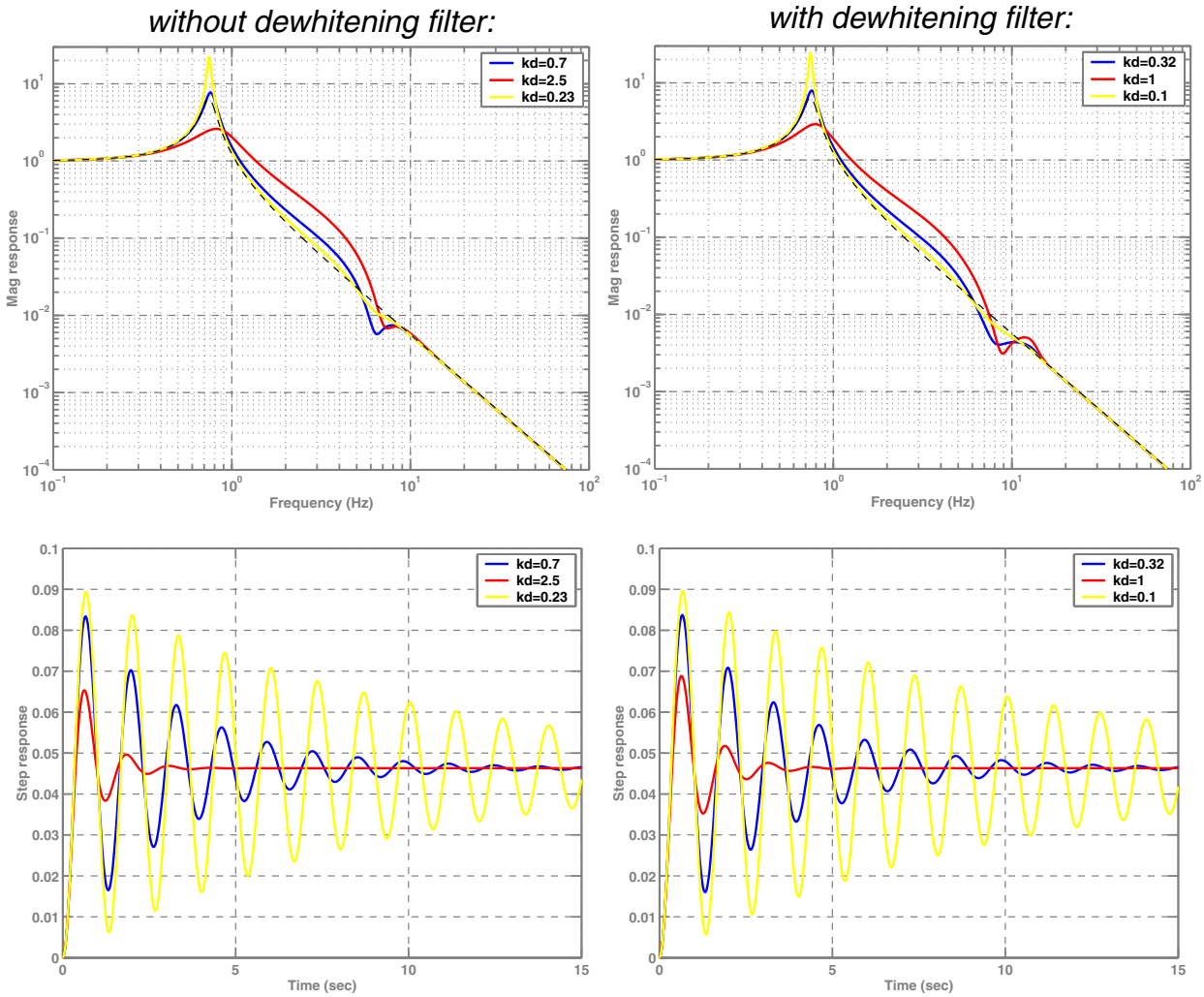

Figure 12. Frequency and step response of the damped LOS, with and without the analog dewhitening filter; the frequency response plots also contain a simple $Q = 7$ resonance for reference. Note that with the dewhitening filter engaged, the damping gain must be reduced by a factor of ~2 to achieve the same pendulum Q (this will be taken care of in the filter coefficients).

4.4.8. Filter implementation

Table 1 lists the filters that are loaded into each of the three filter blocks in the local damping section.

filter number	*filter loaded*	*comment*
15, 18, 21	zero: DC pole: 3 Hz	provides ac-coupling (see section 4.2.)
16, 19, 22	3rd order elliptic low-pass, f_c = 5 Hz, stopband = –40 dB, passband ripple = 0.1 dB	active when hardware dewhitening filters are bypassed
17, 20, 23	2nd order elliptic low-pass, f_c = 3 Hz, stopband = –20 dB, passband ripple = 0.1 dB	nominally always engaged

Table 1: Filters defined for the POS, PIT, & YAW damping sections.

4.5. Output matrix filtering

In the output matrix the POS, PIT & YAW damping signals, and the LSC & ASC feedback signals, are turned into signals for the four individual face coils. With the digital suspension controllers, we have the ability to provide frequency-dependent basis conversions, allowing us to invert or remove any couplings that might exist in the suspension actuation.

The single loop suspension has a built-in coupling between longitudinal and pitch degrees-of-freedom; the coupled equations of motion for arbitrary force and torque (including forces and torques due to local damping) are (see, for example, T960103-00-D, *ASC: Environmental Input to Alignment Noise*, G Gonzalez):

$$\begin{aligned} -\omega^2 x &= -\frac{g}{l}(x - h\theta) + F/M \\ -I\omega^2\theta &= \frac{gh}{l}(x - hL\theta) + N/M \end{aligned} \tag{2}$$

where M is the optic mass, I is the (moment of inertia/mass) about the horizontal axis, h is the pitch distance (distance above the center-of-mass of the wire take-off point), L is the vertical distance from the suspension point to the wire take-off point, $l = L + h$, x is the longitudinal displacement of the center-of-mass with respect to the suspension point, θ is the mirror pitch angle with respect to the vertical, and g is the gravitational acceleration (9.8 m/sec^2).

To remove the force-to-pitch coupling, set $\theta = 0$ and solve for the needed torque:

$$N = -\frac{h}{1 - l\omega^2/g} \cdot F \tag{3}$$

So with D being the vertical distance from a magnet to the center of the optic, the 'Position' coil channels are filtered as follows to cancel the pitch coupling:

$$T(s) = 1 \pm \frac{h/D}{s^2 l/g + 1} = \frac{s^2 l/g + 1 \pm h/D}{s^2 l/g + 1} \rightarrow \frac{(s/\omega_0)^2 + 1 \pm h/D}{(s/\omega_0)^2 + s/(\omega_0 Q) + 1}. \quad (4)$$

where the '+' sign is applied for the upper two coils, and the '–' sign is applied to the lower two coils; in the last expression, $g/l = \omega_0^2$, and a damping term has been added to make the filter stable (and thus realizible; the damping is made small, $Q = 1000$). This assumes that the four coil-magnet actuators all have the same D. Variations between actuators are probably dominated by variations in the force coefficient (due to magnet strength variations, e.g.), which can be accounted for by adjusting gain factors in the output matrix. Hopefully, the filter functions do not have to be individually tailored to each actuator.

To remove the torque-to-position coupling, set $x = 0$ and solve for the needed force:

$$F = \frac{1}{L - (Il/gh)\omega^2} \cdot N. \quad (5)$$

The 'Pitch' coil channels are thus filtered as follows:

$$T(s) = 1 \pm \frac{D}{(Il/gh)s^2 + L} = \frac{(Il/gh)s^2 + L \pm D}{(Il/gh)s^2 + L} \rightarrow \frac{(s/\omega_0)^2 + 1 \pm D/L}{(s/\omega_0)^2 + s/(\omega_0 Q) + 1}, \quad (6)$$

where the '+' sign is applied for the upper two coils, and the '–' sign is applied to the lower two coils; in the last expression, $ghL/Il = \omega_0^2$, and a damping term has been added to make the filter stable (and thus realizible; the damping is made small, $Q = 1000$).

Each of these filters is realized with a single second-order-section. The POS filter, eq. 4, is loaded, with appropriate signs, in filters 24, 33, 42, and 51. The PIT filter, eq. 6, is loaded, with appropriate signs, in filters 27, 36, 45, and 54. The filters are nominally defined using the suspension parameters given in Table 3.

Parameter	*Specification*	
	LOS	*SOS*
l	0.4537 m	0.248 m
h	8.9 mm	0.9 mm
I	(1/211) m^2	(1/2400) m^2
D	80.82 mm (104.78 for BS)	24.70 mm

Table 2: Suspension parameters used to define the output matrix filters. The magnets are arranged in a square for all optics except the beamsplitter, which thus has a different D value than the other LOS.

The effect of the position–pitch coupling cancellation has been modeled using the Simulink block diagram shown in Figure 13. This implements eq. 2, and lets us avoid doing lots of algebra. The

model of course predicts that the force-to-pitch and torque-to-position couplings vanish at all frequencies when the cancellation terms of eq. 3 and eq. 5 are included. Some less obvious resultsare shown in Figure 14.

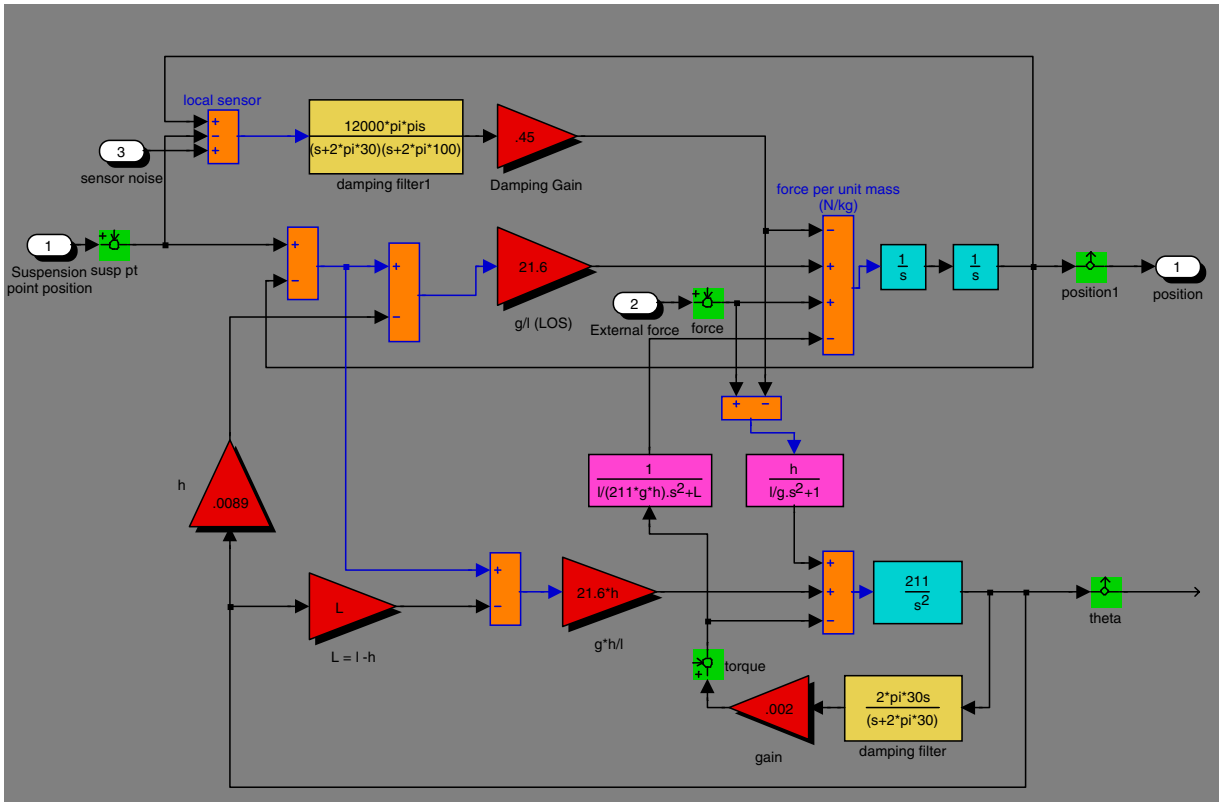

Figure 13. Simulink model used for the coupled longitudinal–pitch pendulum, realizing eq. 2. The magenta blocks contain the cross-coupling cancellation functions. For simplicity, the active damping path contains a velocity factor only (up to 30 Hz), and not the sensor noise low-pass filtering.

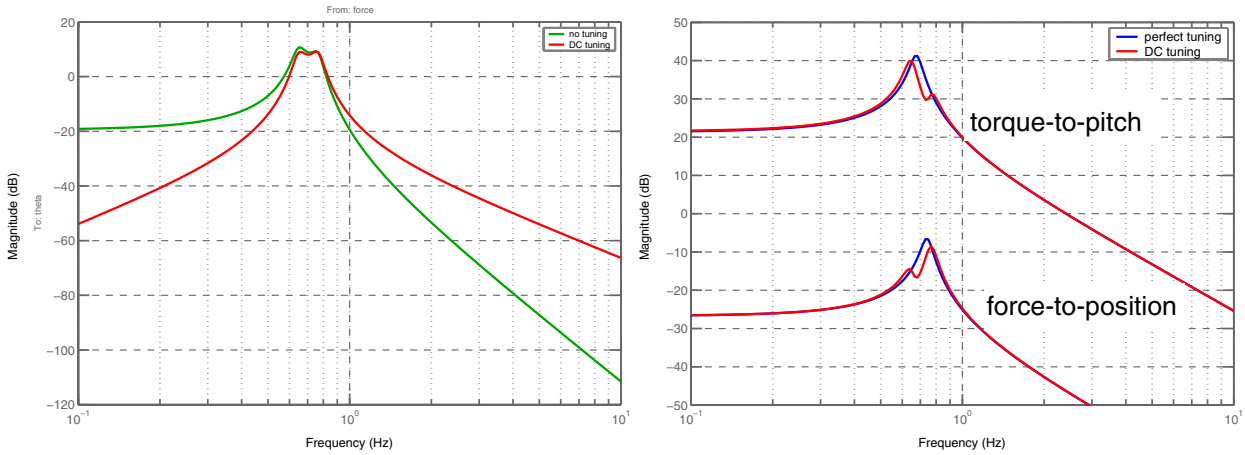

Figure 14. Transfer functions obtained using the Simulink model of Figure 13. Left: Mag response of force (applied to center-of-mass) to pitch angle (theta), with no compensation torque applied (green) and with a constant torque factor applied to eliminate the DC coupling (red), as is done in practice with the analog suspension controllers. While this tuning removes the DC coupling, it still leaves a substantial coupling around the pendulum eigenfrequencies, and increases the coupling at higher frequencies; with the frequency-dependent torque compensation shown in Figure 13, the model indicates the coupling is essentially zero at all frequencies. Right: Mag response of torque-to-pitch angle (upper curves) and force-to-position (lower curves), with DC cross-coupling compensation (red) and with the ideal frequency-dependent compensation (blue); with DC-only tuning, both eigenmodes show up in each drive, whereas with ideal tuning only the intended eigenmode is excited.

4.6. Coil output filtering

The filter banks for the four face coil outputs contain filters to compensate the response of the coil drivers, as listed in Table 3.

filter number	*filter loaded*	*comment*
60, 63, 66, 69	pole: 2.2 Hz zero: 100 Hz	inverse of the additional coil driver filter in ACQUIRE mode; turned ON in ACQUIRE mode
61, 64, 67, 70	zero: 4.4 Hz pole: 30 Hz	inverse of the coil driver in RUN mode; always ON

Table 3: Filters defined for the (UL, LL, UR, LR) coil outputs.